J Craniofac Genet Dev Biol 1997; 17:112–120
Printed in the United States of America—

Journal of Craniofacial Genetics and Developmental Biology
ISSN 0742-3098

Finite element morphometry of the midfacial complex in subjects with Angle's class III malocclusions

Singh GD, McNamara Jr. JA, Lozanoff S: Finite element morphometry of the midfacial complex in subjects with Angle's class III malocclusions. J Craniofac Genet Dev Biol 1997; 17:112–120. © Munksgaard, Copenhagen

Abstract: The purpose of this study was to determine whether the morphology of the midface differed in normal (Class I) and midfacially-retrognathic (Class III) prepubertal subjects, and to localize differences morphometrically. Lateral cephalographs of 133 European-American children between 5–11 years of age were traced and average geometries, scaled to an equivalent size, were generated based upon seven nodes (pterygoid point, PTS; rhinion, RO; posterior nasal spine, PNS; midpalatal point, MPP; anterior nasal spine, ANS; subspinale, A; and prosthion, Pr). The samples also were subdivided into seven age- and sex-matched groups for morphometric comparisons. Procrustes analysis indicated that the overall midfacial configurations differed statistically ($P < 0.05$). Therefore, a color-coded finite element (FEM) program was used to localize differences in morphology graphically. Comparing Class I and Class III groups for size-change, FEM revealed that negative allometry was evident in the posterior half of the midfacial configuration localized between PTS, PNS, and MPP. The anterior half was more isotropic, however, but the anterior-most aspect of the configuration between Pr and RO showed some positive allometry particularly in the premaxillary and incisor regions. For shape-change, major differences in shape over the entire midface were not as evident, with an isotropic midfacial morphology for normal and Class III subjects. It is concluded that an identifiable pattern of deformation is evident for the Class III subjects during the prepubertal growth period. Therefore, midfacial retrognathia associated with Class III malocclusions results, at least in part, from deficient anteroposterior elongation of the midfacial complex allied with deformation of the premaxillary region.

G.D. Singh,[1] J.A. McNamara Jr.,[2] and S. Lozanoff[3]

[1]Department of Dental Surgery and Periodontology, University of Dundee, Scotland, United Kingdom; [2]Department of Orthodontics and Pediatric Dentistry, University of Michigan, Ann Arbor, Michigan; [3]Departments of Anatomy and Reproductive Biology and of Surgery, University of Hawaii, Manoa, Hawaii

Key words: facial – morphology – retrusion

Address reprint requests to Dr. G.D. Singh, Department of Dental Surgery and Periodontology, Dundee Dental Hospital and School, University of Dundee, Park Place, Dundee DD1 4HR, Scotland, United Kingdom. E-mail:g.d.singh@dundee.ac.uk

Introduction

Class III malocclusions may exhibit midfacial sagittal deficiency with or without mandibular excess [Vardimon et al., 1990], therefore the choice of treatment of children with developing skeletal Class III malocclusions has always posed a dilemma [Nanda, 1980]. It has been suggested that there may be an association between facial morphology and malocclusions [Siriwat and Jarabak, 1985]. Martone et al. [1992] consider that Class III malocclusions' sub-groupings are related to head-form type with characteristic morphologic features. For example, in Class III cases the capacity of the oral cavity is thought to be larger than in Class I cases [Yamada, 1990]. This morphologic difference presumably is due to a larger mandibular capacity since no significant differences in maxillary capacity or palatal morphology were found [Yamada, 1990]. But resolution of this complex issue has not been reached; sagittal and vertical, dental and skeletal intermaxillary malrelationships are only partly reflected in the face [Bittner and Panchera, 1990]. Dibbets [1996], however, suggests that the cranial base provides the framework for the maxilla and consequently, in juveniles, the midface above anything else creates the characteristic difference between the Angle Class I and Class III types.

This paper aims to provide evidence for the theory that deficient anteroposterior elongation of the midfacial complex is a factor associated with the development of Class III malocclusions. The analysis will test the hypothesis that principal dilations in the midface occur using FEM and reflect deficient anteroposterior elongation in Class III configurations when Class I and Class III subjects are compared. Therefore, this study will determine sites of developmental discrepancy within the midface from clinical data sets of normal (Class I) and Class III subjects, and correlate these with the appearance of midfacial retrognathia associated with Class III malocclusions. Rejection of the null hypothesis (that there should be no significant skeletal difference between the Class III occlusal type and the Class I control group) will imply differential morphogenesis in craniofacial regions other than the midface. The resultant FEM maps will suggest areas with divergent growth activities, leading to further experimental analyses using animal models of Class III malocclusions [Lozanoff et al., 1994]. Therefore, application of this methodology in the analysis of midfacial morphology may lead to a clearer understanding of the developmental mechanisms responsible for final midfacial form.

Materials and Methods

After obtaining appropriate consent, 133 lateral cephalographs of untreated children of European-American descent aged between 5–11 years were selected. Seventy-three cephalographs of the untreated subjects exhibited an Angle's Class III molar occlusion [Guyer et al., 1986], while the other 60 cephalographs displayed an untreated Angle's Class I molar occlusion. The deployment of approximately equal numbers of male and female subjects permitted the construction of seven age- and sex-matched groups from the total sample. Therefore, when the total sample was decomposed in an age-wise fashion, there were about 20 subjects per age group (10 Class I, 10 Class III) with approximately equal numbers of male and female children in each group, and initial statistical analyses showed no significant differences in this regard. The chronological age was assumed to match developmental age in this study since carpal radiographs were unavailable. All subjects included in the study sample had a negative history of airway problems and no obvious vertical skeletal problems. The magnification of each cephalograph was standardized to 8%. It was presumed that all radiographs were taken from subjects exhibiting left-right symmetry and that the central x-ray passed along the transmeatal axis while the teeth were in occlusion.

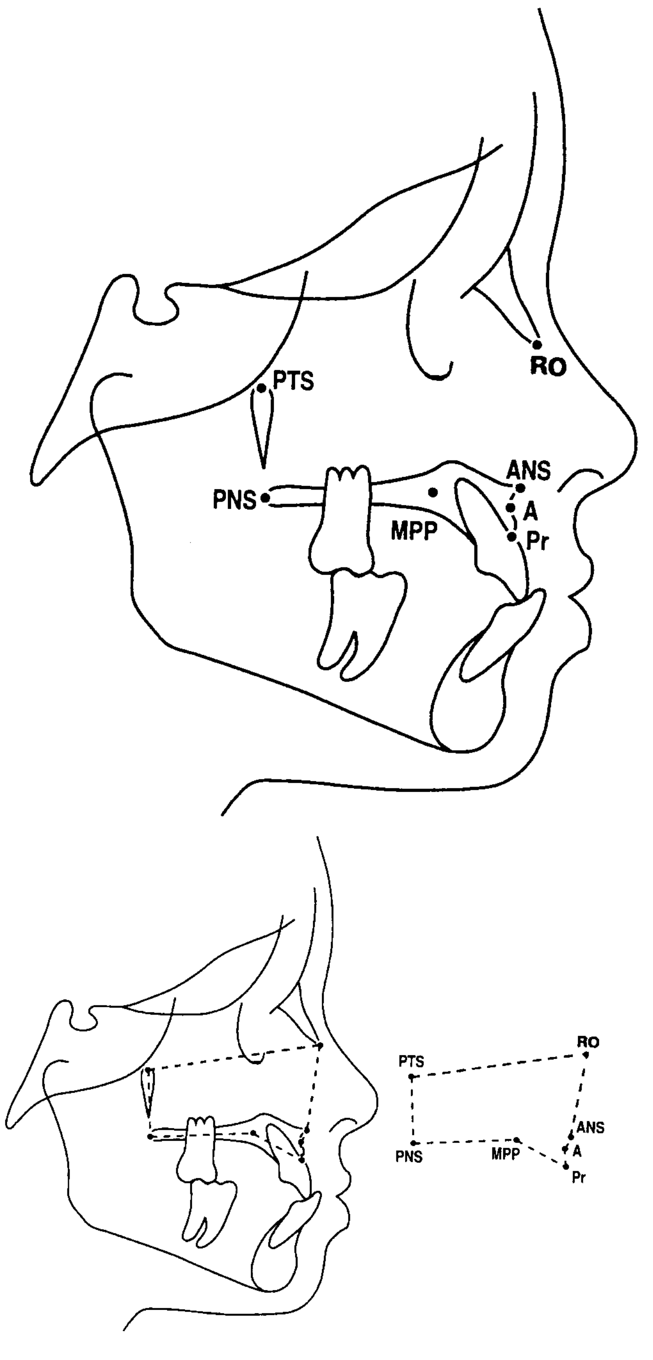

Fig. 1. **a:** Homologous landmarks employed for the construction of a seven-noded geometry to define the midfacial complex. A, Subspinale (point of maximum concavity inferior to the anterior nasal spine on maxillary alveolus). ANS, Anterior nasal spine (anterior-most point on anterior nasal spine). MPP, Midpalatal point (midpoint between outlines of the nasal and oral palatal surfaces). RO, Rhinion (inferior-most point on tip of nasal bone). PNS, Posterior nasal spine (posterior-most point on posterior nasal spine). Pr, Prosthion (antero-inferior point of maxillary incisor alveolus). PTS, Pterygoid point (superior-most point on outline of pterygoid fissure). **b:** Midfacial geometry derived from the seven homologous landmarks employed superimposed on a tracing of a Class III cephalograph, and shown separately. A, subspinale; ANS, anterior nasal spine; MPP, midpalatal point; RO, rhinion; PNS, posterior nasal spine; Pr, prosthion; PTS, pterygoid point.

Table 1. Homologous landmarks digitized from lateral cephalographs[a]

A	Subspinale:	Point of maximum concavity inferior to the anterior nasal spine on maxillary alveolus
ANS	Anterior nasal spine:	Anterior-most point on anterior nasal spine
MPP	Midpalatal point:	The point midway between the outlines of the nasal and oral palatal surfaces
RO	Rhinion:	Inferior-most point on tip of nasal bone
PNS	Posterior nasal spine:	Posterior-most point on posterior nasal spine
Pr	Prosthion:	Antero-inferior point of maxillary incisor alveolus
PTS	Pterygoid point:	Superior-most point on lateral outline of pterygoid fissure

[a]These landmarks were employed to construct seven-noded midfacial geometries for Procrustes and FEM analyses.

Each cephalograph was traced on frosted acetate film (0.03" thick) and checked by one investigator (GDS). Seven homologous landmarks of the midfacial complex were identified and digitized (Fig. 1a and Table 1), employing appropriate software and a digitizing tablet (Numonics, Inc., Montgomeryville, PA). The rationale of selection was that preference was given to landmarks that encompass midfacial developmental sites and were located in the mid-sagittal plane where possible [Varjanne and Koski, 1982; Bhatia and Leighton, 1994]. Any landmarks that showed a discrepancy of >1% on duplicate digitization were deemed to be identified unreliably and were excluded from the final analyses.

The average midfacial configuration of Class I subjects was computed by using a Procrustes analysis [Singh et al., 1997a] and this was compared to the average Class III configuration. The Procrustes analysis is necessary to provide a measure of discrimination between groups, independent of the clinical diagnosis, but bivariate statistical analyses were undertaken on these data also. The total samples were subdivided in an age-wise fashion to determine whether the geometries were significantly different at a particular age. In addition, these average geometries were subjected to a FEM routine [Lozanoff and Diewert, 1989; Singh et al., 1997a,b] that incorporated a spline function algorithm [Bookstein, 1991] for interpolating strains internal to the anatomical landmark coordinates. The choice of Bookstein's interpolation [Bookstein, 1991] was arbitrary since there is no biological justification for the deployment of a spline function, and it is for this reason that other approaches were included in this study. The software was written in C language and implemented on an Amiga 3000. The total Class I configuration was taken as the initial geometry, and this configuration was compared to the Class III mean. The geometries for each age grouping were also compared. Therefore, eight comparisons were generated in total. Size-change variables were computed as the product of the principal extensions, while shape-change measures were calculated as the ratio of the greater divided by the lesser principal extension [Lozanoff and Diewert, 1986; Singh et al., 1997a,b]. These values were computed for at least 2,000 points per geometry for graphical display but since no biological points internal to the seven-noded geometry were used, only values at homologous landmarks were tabulated. A log-linear interpolation of the size- and shape-values was used to generate a color map. These form-change measures were then color-mapped into each Class I midfacial configuration to provide graphical displays of geometrical change for each total and age-wise comparison.

Results

Initial Procrustes results based upon the average normal (Class I) and midfacially-retrognathic (Class III) seven-noded geometries, scaled to an equivalent size, indicated that the overall mean configurations were statistically different ($P < 0.05$: TF; Table 2). When the total sample was subdivided into age-matched groups, however, not all age groups maintained statistical significance (Table 2). The results of bivariate analyses by utilizing nine linear and six angular measurements indicated that although the overall midfacial configurations differed statistically, only four of the linear (PNS-MPP, MPP-ANS, A-Pr, and PTS-RO) and only two of the angular parameters (PTS-RO-ANS and ANS-A-Pr) tested were significantly different ($P < 0.05$). Comparing normal and midfacially-retrognathic groups for size- and shape-change, finite element analysis revealed size reduction was evident at nodes PTS, MPP, and PNS but that size increase was evident at nodes RO, ANS, A, and Pr. Minor shape-change at these nodes also was detected (Table 3).

For the 5-year-old group, negative allometry (13% reduction in size) was visible in the posterior half of the midfacial configuration localized between PTS, PNS, and MPP (Fig. 2a). While the anterior half showed little sign of size reduction, however, the maxillary incisor alveolus between A and Pr showed a 30% increase in size. For shape-change (Fig. 3a), the midfacial configuration was highly isotropic (uniform shape-change) about its centroid region, but minor anisotropy (heterogeneic shape-change) was evident at the anterior aspect of the configuration, localized in the region of the ANS.

Table 2. Procrustes analysis of mean midfacial configurations of normal (Class I) and midfacially-retruded (Class III) subjects[a]

Age (years)	5	6	7	8	9	10	11	TF
Residual	0.0008	0.0012	0.0019	0.0003	0.0012	0.0011	0.0007	0.0006
F value	0.8310	0.7810	1.4826	0.3624	2.1346	1.0688	0.7386	1.8685
P value	0.05	N.S.	0.01	N.S.	<0.01	<0.01	N.S.	<0.05

[a]TF represents the total combined Class I and Class III comparison that is significantly different at the $P < 0.05$ level. When the total sample is decomposed into age sub-groups, age 7, 9, and 10 years maintain statistical difference, while at age 5 the Class I and Class III comparison marginally fails to reach statistical significance at the $P < 0.05$ level. Sub-groups at ages 6, 8, and 11 years are statistically not sigificant (N.S.).

For the 6-year-old group, negative allometry (10%) was visible in the posterior two thirds of the midfacial configuration, extending beyond the MPP (Fig. 2b). The anterior third of the geometry showed more uniformity in size, but the maxillary incisor alveolus between A and Pr showed a 20% increase in size. For shape-change, the midfacial configuration was isotropic between ANS and PNS with evidence of some anisotropy (Fig. 3b). Anisotropic changes were evident for the maxillary alveolus, particularly localized in the Pr region.

For the 7-year-old group, negative allometry (22%) was restricted to the postero-inferior quadrant of the midfacial configuration between the PNS and MPP (Fig. 2c). While the mid-region of the geometry exhibited little sign of size reduction, however, the anterior aspect was positively allometric with an increase in size of 20% between ANS and RO. For shape-change (Fig. 3c), the midfacial configuration was isotropic about its centroid region but minor anisotropy was evident posteriorly between PNS and PTS, and more specifically localized anteriorly with its epicenter in the region of subspinale.

The 8-year-old group was remarkably similar to the 5-year-old group for size-change. Negative allometry (7%) was visible posteriorly, while the anterior half showed isometry (Fig. 2d). The maxillary incisor alveolus between A and Pr showed positive allometry (26%). For shape-change, however, the 8-year-old group midfacial configuration was predominantly isotropic (Fig. 3d) but some minor heterogeneic changes were localized anteriorly in the vicinity of ANS.

For the 9-year-old group, negative allometry (10%) was evident in the posterior half of the midfacial configuration localized between the PTS, PNS, and the MPP (Fig. 2e). However, the anterior half was more isotropic but the anterior aspect of the configuration between Pr and A showed some positive allometry (14% increase in size). For shape-change (Fig. 3e), the 9-year-old group was very similar to the 8-year-old midfacial configuration. It was predominantly isotropic with minor anisotropy anteriorly, particularly localized at Pr.

Table 3. FEM analysis comparing Class I and Class III midfacial nodal values for size- and shape-change[a]

Size						
PTS	RO	ANS	MPP	PNS	A	Pr
0.928	1.058	1.072	0.984	0.898	1.093	1.160
Shape						
PTS	RO	ANS	MPP	PNS	A	Pr
1.001	1.001	1.000	1.000	1.000	1.002	1.004

For the 10-year-old group, the pattern of size-change was similar to the 9-year-old configuration. Negative allometry (12%) was evident in the posterior half of the geometry but the anterior half was more isometric (Fig. 2f). The anterior aspect of the configuration between Pr and A showed some positive allometry (around Pr; 22% increase in size). For shape-change (Fig. 3f), the midfacial configuration was less isotropic about its centroid region with heterogeneic changes at the superior and antero-inferior aspects of the configuration, particularly localized in the region of subspinale.

The 11-year-old midfacial configuration was similar to the 7-year-old geometry for size-change analysis. Negative allometry (15%) was restricted to the posterior third of the midfacial configuration between the PTS, PNS, and MPP (Fig. 2g). While the mid-region was more isometric, however, the anterior aspect was positively allometric with an increase of 14% near ANS. For shape-change (Fig. 3g), the 11-year-old midfacial configuration was similar to the 9-year-old geometry. It was predominantly isotropic with anisotropy restricted to an anterior region with an epicenter localized at subspinale.

Comparing the overall normal and midfacially-retrognathic groups, localized size-changes in the midfacial complex were evident also (Fig. 2h). Negative allometry (12%) was seen in the posterior half of the configuration localized between PTS, PNS, and MPP. The anterior half was more isometric, however, and the anterior-most aspect of the configuration between Pr and A showed some positive allometry (18% increase in size between Pr and A). For shape-change (Fig. 3h), major differences in shape over the entire midface were not as evident, with predominantly isotropic configurations. Minor regions of anisotropy,

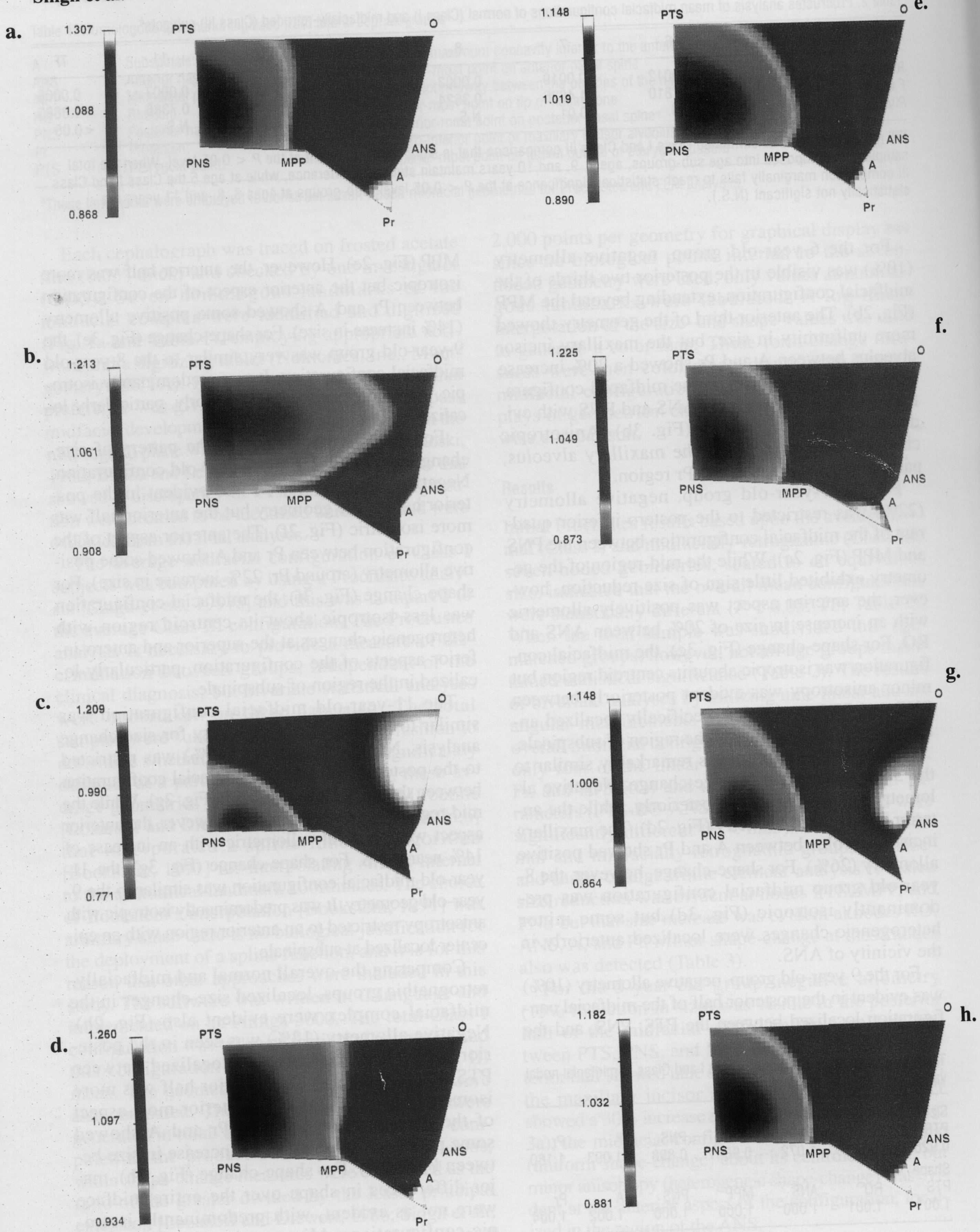
a.
1.307
1.088
0.868
PTS
O
PNS
MPP
ANS
A
Pr
b.
1.213
1.061
0.908
PTS
PNS
MPP
ANS
Pr
c.
1.209
0.990
0.771
PTS
O
PNS
MPP
ANS
A
Pr
d.
1.260
1.097
0.934
PTS
O
PNS
MPP
ANS
A
Pr
e.
1.148
1.019
0.890
PTS
O
PNS
MPP
ANS
A
Pr
f.
1.225
1.049
0.873
PTS
O
PNS
MPP
ANS
A
Pr
g.
1.148
1.006
0.864
PTS
O
PNS
MPP
ANS
A
Pr
h.
1.182
1.032
0.881
PTS
O
PNS
MPP
ANS
A
Pr

however, were noticeable in the anterior third of the configuration, reaching a maximum of <1% in the A and Pr regions.

Discussion

Motoyoshi et al. [1989] employed four-noded, three-dimensional FEM in the prediction of normal craniofacial growth and suggested that FEM is a method of great significance for obtaining new findings on craniofacial growth. The purpose of this present study was to determine how the midfacial complex differs in normal and Class III subjects that exhibit a deficient midfacial profile in the sagittal plane by using FEM, and to derive developmental hypotheses that would account for any apparent growth differences. Class III malocclusions may be categorized in several ways: for example, by using incisor relationships, cephalometric parameters (i.e., overjet, angle ANB, distance from A point to nasion perpendicular, etc.), or molar occlusion. Only the latter definition was employed in this particular study and, although the problem with using a dental classification as opposed to a skeletal one is that molar malrelationships can be found in any of three skeletal types of discordance, our cross-sectional study employed a generalized Procrustes procedure [Singh et al., 1997a] to provide a measure of discrimination between the two groups independent of the clinical diagnosis.

Although this current study was restricted to two dimensions, we have been able to report findings that confer well with previous studies. For example, this study demonstrates that localized size-change is greater than localized shape-change, and this finding is in accord with earlier morphometric analyses of craniofacial growth in humans using FEM [e.g., Richtsmeier and Cheverud, 1986]. But, geometric concavities remain a problem for landmark approaches. The accuracy for concavities was not tested in this study because the concavities of the geometric configurations obtained (such as in the region of ANS-A-Pr) were not severe. The deployment of outline procedures like Fourier analysis, however, may be useful for future investigations as the color figures generated were based upon seven homologous nodes, and the internal representation of strains were not based upon internal, biologically-derived points. Despite these drawbacks, meaningful findings relating to midfacial growth and developmental hypotheses were obtained.

During growth, anterior facial height ratios remain relatively constant in children and adults with normal occlusion but the potential for changes in the ratio of the posterior facial height is greater [Chang et al., 1993]. In our study, it appears that the posterior half of the midfacial complex shows size diminution in the Class III subject, and it is conceivable that this reduction in midfacial dimensions contributes to a smaller maxillofacial complex that would appear retrognathic with respect to an orthognathic mandible. In *Macaca fasicularis* monkeys, Vardimon et al. [1990] reported that protraction of the maxillary complex was initiated at the pterygomaxillary fissure with additional contributions from the zygomatico-maxillary, transverse, and premaxillary sutures when these animals were subjected to functional orthopedic appliance therapy. These findings are in accord with the developmental hypothesis that growth deficiencies at the pterygoid and maxillary sutures do not permit forward midfacial growth commensurate with mandibular development, but sutures are adaptive rather than directive, and the contribution of synchondroses is also thought to be minimal during the age range of

Fig. 2. Size-change color maps transforming the mean Class I geometry into the mean Class III configuration. The color figures were generated based upon seven homologous nodes, and the internal representation of strains were not based upon internal, biologically-derived points. A log-linear interpolation of the size-values was used to generate the color maps; therefore, the scale bar differs for each geometry as the FEM program optimizes the color range for each graphical display. **a:** Five year-old midfacial configuration. Negative allometry is visible in the posterior half of the configuration between PTS, PNS, and MPP but maxillary incisor alveolus shows an increase in size. **b:** Six-year-old midfacial configuration. Negative allometry is visible in the posterior two thirds of the midfacial configuration, extending beyond the MPP. The anterior third shows more uniformity in size, but the maxillary incisor alveolus between A and Pr shows an increase in size. **c:** Seven-year-old midfacial configuration. Negative allometry is restricted to the postero-inferior quadrant of the midfacial configuration between the PNS and MPP. The mid-region exhibits size reduction but the anterior aspect is positively allometric with increase in size between ANS and RO. **d:** Eight-year-old midfacial configuration. Posterior half of the configuraiton is negatively allometric, while the anterior half shows isometry. Maxillary incisor alveolus is positively allometric. **e:** Nine-year-old midfacial configuration. Negative allometry is evident in the posterior half of the midfacial configuration localized between the PTS, PNS, and the MPP. The anterior half is more isotropic and the anterior aspect of the configuration between Pr and A shows positive allometry. **f:** Ten-year-old midfacial configuration. Negative allometry is evident in the posterior half of the geometry but the anterior half is more isometric. The anterior aspect of the configuration between Pr and A shows positive allometry around Pr. **g:** Eleven-year-old configuration. Negative allometry is restricted to the posterior third of the midfacial configuration between the PTS, PNS, and MPP, while the mid-region is more isometric. The anterior aspect, however, is positively allometric. **h:** Overall comparison of normal and midfacial-retrognathic midfacial configuraiton for size-change. Negative allometry is seen in the posterior half of the configuration localized between PTS, PNS, and MPP. The anterior half is more isometric, however, and the anterior-most aspect of the configuration between Pr and A shows positive allometry.

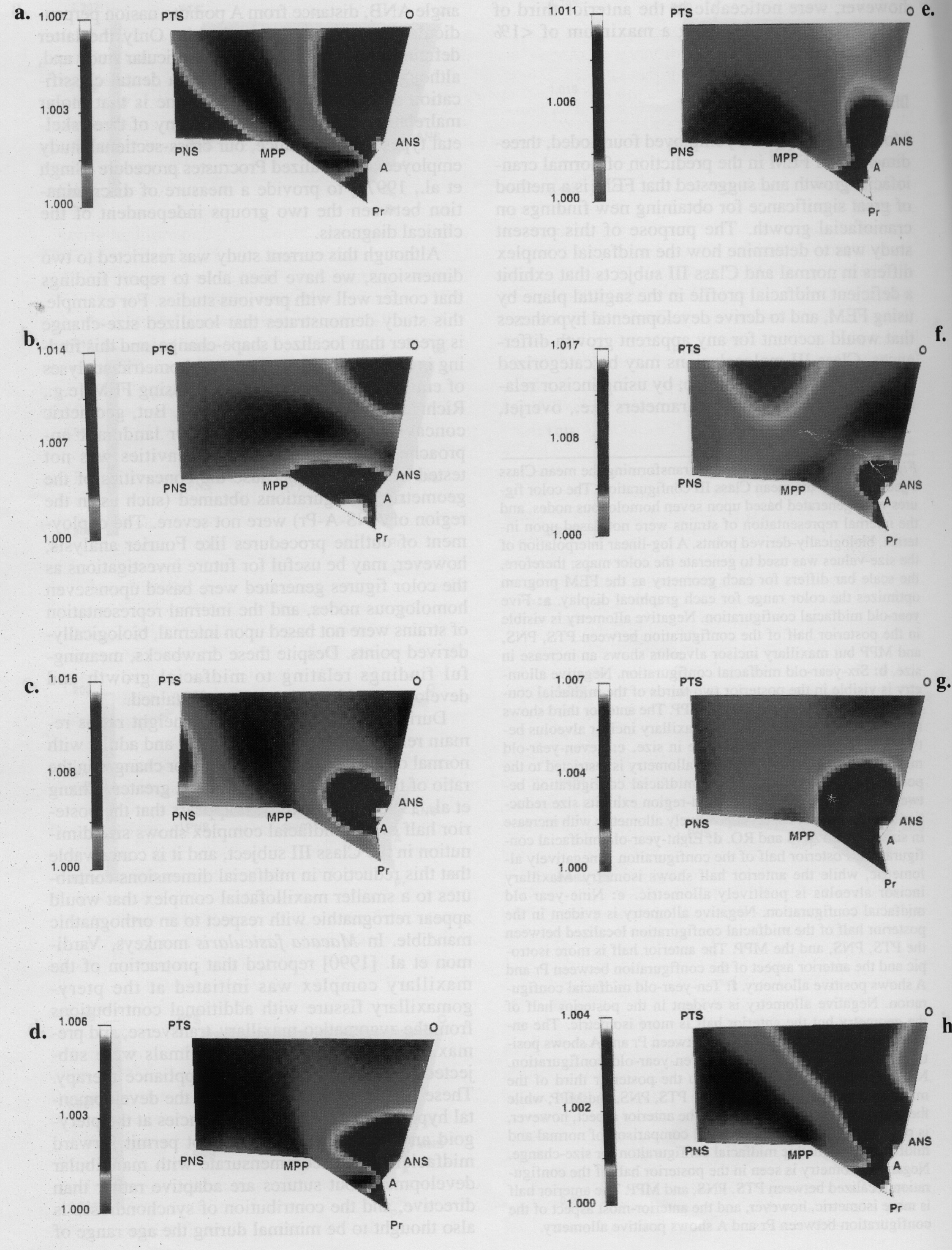
a.
1.007
1.003
1.000
PTS
O
PNS
MPP
ANS
A
Pr
b.
1.014
1.007
1.000
PTS
O
PNS
MPP
ANS
A
Pr
c.
1.016
1.008
1.000
PTS
O
PNS
MPP
ANS
A
Pr
d.
1.006
1.003
1.000
PTS
O
PNS
MPP
ANS
A
Pr
e.
1.011
1.006
1.000
PTS
O
PNS
MPP
ANS
A
Pr
f.
1.017
1.008
1.000
PTS
O
PNS
MPP
ANS
A
Pr
g.
1.007
1.004
1.000
PTS
O
PNS
MPP
ANS
A
Pr
h.
1.004
1.002
1.000
PTS
O
PNS
MPP
ANS
A
Pr

the subjects in this study. Therefore, growth sites and mechanisms responsible for midfacial insufficiency require further elucidation. Vardimon et al. [1994], however, suggested that the sutural response was composed of disarticulation and osteogenesis at the palatomaxillary and pterygopalatine sutures in monkeys. Therefore, our study localized the pterygomaxillary fissure as a developmental site that could contribute toward midfacial deficiency and parallels the study of Tanne et al. [1995], who suggested that the center of rotation of the nasomaxillary complex is located on the posterosuperior ridge of the pterygomaxillary fissure.

It is possible that rapidly growing facial sutures may exhibit compensatory midfacial growth as alluded to by studies on rabbits [Mooney et al., 1992]. Further evidence for this notion arises from the work of Takada et al. [1993] who reported that increases in maxillary length (Ptm-A) are demonstrable in prepubertal females treated with maxillary protraction headgear. That midfacial compensation is a likely developmental mechanism stems from an analysis of the premaxillary region in our study. Overall, positive allometry (10–15%) was evident in the premaxillary region (Fig. 2h), and this pattern of compensation is supported by the finding that no size diminution was found in the anterior half of the midface, particularly between MPP and A. Therefore, while the posterior half of the midfacial skeleton exhibited size reductions, this diminution was offset, at least in part, by an increase further anteriorly, but the developmental potential of the premaxillary region appears to less significant than the palatomaxillary and pterygopalatine sutures, since these subjects exhibited a retrognathic midfacial profile. Nevertheless, a translatory contribution from concomitant growth at the spheno-ethmoidal synchondrosis may have aided the anterior displacement of the midfacial skeleton during morphogenesis.

The vertical relationship, i.e., dolichofacial (long-faced) or brachyfacial (short-faced), is of particular importance in the formulation of orthodontic treatment planning [Collett and West, 1993]. When analyzing our results for shape-change, we found that on the whole the midfacial configurations were largely isotropic. This finding suggests that the nature of the shape-change is homogeneous and does not have a particular directionality in either the horizontal or vertical axes. Anisotropy when present, however, usually was restricted to the maxillary alveolar region and incisor regions. Concomitant to this regionalized anisotropy was positive allometry (15–30%). These findings suggest that morphological change in the maxillary incisors, presumably dental compensation, also is a feature of the Class III subject. Indeed, when treating skeletal sagittal maxillomandibular disproportions, alveolar inclinations have to be taken into account. They are either compensatory or aggravate the basal bone discrepancies [Fleury et al., 1994]. It appears that in this particular study relative maxillodental compensation is identifiable.

The contribution of other craniofacial structures has not been investigated in this current study. With respect to cranial base, Gasson and Lavergne [1977a] found no connection between variation in maxillary rotation and growth of the cranial base. In studies of the cranial base in isolation, Singh et al. [1997a,b,c] suggested deficient orthocephalization in subjects with Class III malocclusions. With respect to the mandible, Gasson and Lavergne [1977a] reported a correlation between maxillary rotation and mandibular rotation of the corpus, and condylar growth direction. Gasson and Lavergne [1977b] suggest that the interaction between maxillary and mandibular rotations plays an important role in the vertical and sagittal relationships of the jaws. Therefore, a comprehensive study of other craniofacial components of Class III malocclusions is warranted.

In summary, this current study localized shape-

Fig. 3. Shape-change transforming the mean Class I geometry into the mean Class III configuration. The color figures were generated based upon seven homologous nodes, and the internal representation of strains were not based upon internal, biologically-derived points. A log-linear interpolation of the size-values was used to generate the color maps; therefore, the scale bar differs for each geometry as the FEM program optimizes the color range for each graphical display. **a:** Five year-old midfacial configuration is highly isotropic about its centroid region, but minor anisotropy is evident at the anterior and posterior aspects of the configuration, localized particularly in the region of ANS. **b:** Six-year-old midfacial configuration is isotropic between ANS and PNS with evidence of anisotropic changes in the maxillary alveolus, particularly localized in the Pr region. **c:** Seven-year-old midfacial configuration is isotropic about its centroid region but minor anisotropy is evident posteriorly between PNS and PTS, and more specifically localized anteriorly with its epicenter in the region of subspinale. **d:** Eight-year-old midfacial configuration is predominantly isotropic with minor heterogeneic changes localized anteriorly in the vicinity of ANS. **e:** Nine-year-old midfacial configuration is predominantly isotropic with minor anisotropy anteriorly, particularly localized at Pr. **f:** Ten-year-old midfacial configuration is less isotropic about its cnetroid region with heterogeneic changes at the superior and antero-inferior aspects of the configuration, particularly localized in the region of subspinale. **g:** Eleven-year-old configuration is predominantly isotropic with anisotropy restricted to an anterior region with an epicentre localized at subspinale. **h:** Overall comparison of normal and midfacial-retrognathic midfacial configuration for shape-change. Major difference in shape over the entire midface are not evident, producing a predominantly isotropic configuration. Minor regions of anisotropy, however, are noticeable in the anterior third of the configuration, localized in the ANS, A, and Pr regions.

and size-changes in two different occlusal groups that are defined by their maxillomandibular discrepancy. The subjects constituting the Class III grouping (midfacially-retrognathic subjects) exhibited a particular pattern of deformation by using finite element analysis. This pattern of deformation may influence the final morphology of the midface in the appearance of Class III malocclusions. Despite the findings reported for the midfacial complex in this current study, the biological range of allometry is a question that FEM alone cannot answer. The FEM findings, as presented here, only describe the statistical differences rendered through Procrustes analysis. In order to determine the significance of the allometric changes, regression analysis would have to be employed, and this will be considered in a future study. Therefore, the analysis presented here represents a step in the development of algorithms that might lead to maxillomandibular growth outcome prediction.

Acknowledgments

This work was supported by the Wellcome Trust (UK) and the Medical Research Council (Canada).

References

Bittner C, Pancherz H: Facial morphology and malocclusions. Am J Orthod Dentofac Orthop 97:308–315, 1990.

Bhatia SN, Leighton BC: "A Manual of Facial Growth: A Computer Analysis of Longitudinal Cephalometric Growth Data." Oxford: Oxford University Press, 1994.

Bookstein FL: "Morphometric Tools for Landmark Data: Geometry and Biology." Cambridge: Cambridge University Press, 1991.

Chang HP, Kinoshita Z, Kawamoto T: A study of the growth changes in facial configuration. Eur J Orthod 15:493–501, 1993.

Collett AR, West VC: Terminology of facial morphology in the vertical dimension. Aust Dent J 38:204–209, 1993.

Dibbets JM: Morphological associations between the Angle classes. Eur J Orthod 18:111–118, 1996.

Fleury JE, Deboest D, Maffre N, Lacour M, Deneuville O, Assaad C: Fundamental elements of maxillofacial orthodontics in the treatment of sagittal maxillo-mandibular disproportion. Rev Stomatol Chir Maxillofac 95:147–150, 1994.

Gasson M, Lavergne J: The maxillary rotation: Its relation to the cranial base and the mandibular corpus: An implant study. Acta Odont Scand 33:89–94, 1977a.

Gasson M, Lavergne J: Maxillary rotation during human growth: Annual variation and correlations with mandibular rotation: A metal implant study. Acta Odont Scand 35:13–21, 1977b.

Guyer EC, Ellis E, McNamara JA Jr, Behrents RG: Components of Class III malocclusions in juveniles and adolescents. Angle Orthod 56:7–30, 1986.

Lozanoff S, Diewert VM: Measuring histological form change with finite element methods. Am J Anat 177: 187–201, 1986.

Lozanoff S, Diewert VM: A computer graphics program for measuring two three-dimensional form change in developing craniofacial cartilages using finite elements. Comp Biomed Res 22:63–82, 1989.

Lozanoff S, Jureczek S, Feng T, Padwal R: Anterior cranial base morphology in mice with midfacial retrusion, Cleft Palate Craniofac J 31:1–12, 1994.

Martone VD, Enlow DH, Hans MG, Broadbent BH Jr, Oyen O: Class I and Class III malocclusions sub-groupings related to headform type. Angle Orthod 62:35–42, 1992.

Mooney MP, Losken HW, Siegel MI, Tsachakaloff A, Losken A, Janosky J: Plate fixation of premaxillomaxillary suture and compensatory midfacial growth changes in the rabbit. J Craniofac Surg 3:197–202, 1992.

Motoyoshi M, Yamazaki T, Inoue Y, Lin M, Namura S: Application of the finite element method to craniofacial growth analysis. 4. Three-dimensional application of tensor analysis. Nippon Kyosei Shika Gakki Zasshi 48:521–534, 1989.

Nanda R: Biomechanical and clinical considerations of a modified protraction headgear. Am J Orthod 78:125–139, 1980.

Richtsmeier JT, Cheverud JM: Finite element scaling analysis of human craniofacial growth. J Craniofac Genet Dev Biol 6:289–323, 1986.

Singh GD, McNamara JA Jr, Lozanoff S: Finite element analysis of the cranial base in subjects with Class III malocclusion. Br J Orthod 24:103–112, 1997b.

Singh GD, McNamara JA Jr, Lozanoff S: Morphometry of the cranial base in subjects with Class III malocclusion. J Dent Res 76:694–703, 1997a.

Singh GD, McNamara JA Jr, Lozanoff S: Thin-plate spline analysis of the cranial base in subjects with Class III malocclusion. Eur J Orthod, 1997c (in press).

Siriwat PP, Jarabak JR: Malocclusion and facial morphology is there a relationship? An epidemiologic study. Angle Orthod 55:127–138, 1985.

Takada K, Petdachai S, Sakuda M: Changes in dentofacial morphology in skeletal Class III children treated by modified maxillary protraction headgear and a chin cup: A longitudinal cephalometric appraisal. Eur J Orthod 15:211–221, 1993.

Tanne K, Matsubara S, Sakuda M: Location of the centre of resistance for the nasomaxillary complex studied in a three-dimensional finite element model. Br J Orthod 22:227–232, 1995.

Vardimon AD, Graber TM, Voss LR, Muller TP: Functional orthopedic magnetic appliance (FOMA) III modus operandi. Am J Orthod Dentofac Orthop 97:135–148, 1990.

Vardimon AD, Graber TM, Stutzmann J, Voss L, Petrovic AG: Reaction of the pterygomaxillary fissure and the condylar cartilage to intermaxillary Class III magnet mechanics. Am J Orthod Dentofac Orthop 105:401–413, 1994.

Varjanne I, Koski K: Cranial base, sagittal jaw relationship and occlusion. Proc Finn Dent Soc 78:179–183, 1982.

Yamada A: A study of the relationship between the capacity of oral cavity proper and skeletal malocclusions. Aichi Gakuin Daigaku Shigakki Shi 28:203–223, 1990.